Predicting the spin-lattice order of frustrated systems from first principles

H. J. Xiang,[1,][*] E. J. Kan,[2] Su-Huai Wei,[3] M.-H. Whangbo,[4] and X. G. Gong[1]

[1]*Key Laboratory of Computational Physical Sciences (Ministry of Education), and Department of Physics, Fudan University, Shanghai 200433, People's Republic of China*

[2]*Department of Applied Physics, Nanjing University of Science and Technology, Nanjing, Jiangsu 210094, People's Republic of China*

[3]*National Renewable Energy Laboratory, Golden, Colorado 80401, USA*

[4]*Department of Chemistry, North Carolina State University, Raleigh, North Carolina 27695-8204, USA*

A novel general method of describing the spin-lattice interactions in magnetic solids is proposed in terms of first-principles calculations. The spin exchange and Dzyaloshinskii-Moriya interactions, as well as their derivatives with respect to atomic displacements, can be evaluated efficiently on the basis of density-functional calculations for four ordered spin states. By taking into consideration the spin-spin interactions, the phonons, and the coupling between them, we show that the ground-state structure of a representative spin-frustrated spinel, $MgCr_2O_4$, is tetragonally distorted, in agreement with experiments. However, our calculations find the lowest energy for the collinear spin ground state, in contrast to previously suggested noncollinear models.

I. INTRODUCTION

Spin-frustrated systems[1–3] have recently attracted considerable attention because of their novel magnetic properties. The geometrically frustrated spin lattice generally leads to numerous degenerate spin configurations. In principle, a strongly frustrated system mostly has no long-range spin order, but the degeneracy can often be lifted by the spin-lattice coupling; a symmetry-lowering lattice distortion gives rise to a long-range magnetic order at low temperature. In the emerging field of multiferroics,[4] it was found that many frustrated magnets (such as $RMnO_3$[5] and RMn_2O_5[6]) display a large magnetoelectric coupling. Magnetic frustration combined with a striking spin-lattice coupling appears to cause their multiferroic properties. In particular, the exchange striction (a kind of spin-lattice coupling arising from the dependence of the symmetric exchange interactions on the atomic positions) is considered to induce the ferroelectricity in some collinear antiferromagnets such as RMn_2O_5.[7] An alternative mechanism of multiferroicity comes from the inverse effect of Dzyaloshinskii-Moriya (DM) interaction[8] (another kind of spin-lattice coupling arising from the dependence of antisymmetric exchange interactions on the atomic positions), which explains the ferroelectricity in many noncollinear spiral magnets such as $RMnO_3$[8–10] and $Ni_3V_2O_8$.[11] A significant contribution of the symmetric $\mathbf{S_i} \cdot \mathbf{S_j}$-type magnetostriction to the ferroelectricity in $RMnO_3$ was also revealed by Mochizuki *et al.*, who estimated the dependence of the nearest-neighbor (NN) ferromagnetic (FM) coupling in $RMnO_3$ on the Mn-O-Mn bond angle in an empirical way.[12] It is clear that a quantitative description of the spin-lattice coupling is desirable for further study of frustrated magnets.

In their pioneering work, Fennie and Rabe[13] developed a first-principles method to calculate the second-order derivatives of the symmetric exchange parameter and the spin-phonon coupling parameter, and they studied the influence of magnetic order on the optical phonons of the geometrically frustrated spinel $ZnCr_2O_4$. However, their work does not fully describe how the spins couple to the lattice[13] and how to predict the spin lattice order in frustrated systems from

first principles is unclear. Here in this work, we propose a general first-principles description of spin-lattice coupling that allows one to efficiently evaluate the symmetric and antisymmetric exchange interaction parameters and their first-order derivatives with respect to atom displacements. As a test of our method, we examined a representative frustrated system, the spinel $MgCr_2O_4$, to find that its ground-state structure is tetragonally distorted with collinear antiferromagnetic (AFM) spin configuration.

In Sec. II, we will describe a method for computing the spin-lattice coupling parameters. The approach for predicting the spin-lattice ground state using the spin-lattice coupling parameters will be discussed in Sec. III. Then we will apply the methods to find the spin-lattice ground state of $MgCr_2O_4$ in Sec. IV. Finally, we will summarize our work in Sec. V.

II. QUANTITATIVE DESCRIPTION OF THE SPIN-LATTICE COUPLING

A. Method for computing the symmetric exchange parameters

Consider a classical Heisenberg spin system, whose energy can be written as $E = E_0 + E_{spin}$, where $E_{spin} = \sum_{\langle i,j \rangle} J_{ij} \mathbf{S}_i \cdot \mathbf{S}_j$ is the spin exchange term with $|\mathbf{S}_i| = S$, and E_0 is the energy due to other interactions (e.g., the lattice elastic energy), which depends on the atom displacements but not the spin orientations. The spin-exchange interactions are short-range interactions and become negligible when the distance between the spin sites i and j is longer than a certain critical distance R_c. Given a supercell large enough so any spin site has no interaction with its neighboring cells, we extract the exchange interactions as follows. Without loss of generality, consider a particular exchange interaction J_{12} between spin sites 1 and 2. The spin Hamiltonian can be written as

$$E_{spin} = J_{12}\mathbf{S}_1 \cdot \mathbf{S}_2 + \mathbf{S}_1 \cdot \mathbf{K}_1 + \mathbf{S}_2 \cdot \mathbf{K}_2 + E_{other}, \quad (1)$$

where $\mathbf{K}_1 = \sum_{i \neq 1,2} J_{1i} \mathbf{S}_i$, $\mathbf{K}_2 = \sum_{i \neq 1,2} J_{2i} \mathbf{S}_i$, and $E_{other} = \sum_{i,j \neq 1,2} J_{ij} \mathbf{S}_i \cdot \mathbf{S}_j$. It should be noted that $\mathbf{K}_1$, $\mathbf{K}_2$, and E_{other} do not depend on the spin directions of sites 1 and 2. Consider the following four collinear spin states (with z as the spin

quantization axis): (i) $S_1^z = S$, $S_2^z = S$; (ii) $S_1^z = S$, $S_2^z = -S$; (iii) $S_1^z = -S$, $S_2^z = S$; (iv) $S_1^z = -S$, $S_2^z = -S$. In these four spin states, the spin orientations for the spin sites other than 1 and 2 are the same. One can easily show that the four states have the following energy expressions:

$$
\begin{aligned}
E_1 &= E_0 + E_{\text{other}} + J_{12}S^2 + K_1 S + K_2 S, \\
E_2 &= E_0 + E_{\text{other}} - J_{12}S^2 + K_1 S - K_2 S, \\
E_3 &= E_0 + E_{\text{other}} - J_{12}S^2 - K_1 S + K_2 S, \\
E_4 &= E_0 + E_{\text{other}} + J_{12}S^2 - K_1 S - K_2 S.
\end{aligned}
\tag{2}
$$

Thus, J_{12} is extracted by the following formula:

$$
J_{12} = \frac{E_1 + E_4 - E_2 - E_3}{4S^2}.
\tag{3}
$$

The total energies of the four states can be calculated using density-functional theory (DFT). The method described above is a kind of mapping analysis[14] that has been used widely to extract the exchange parameters. In the usual mapping process, one usually considers the spin states with small supercells to reduce computational demand. Here the use of a large supercell has the advantage that the extraction of a particular exchange interaction is independent of other exchange interactions and all total energies are computed using the same supercell. In principles, the accuracy of the exchange parameters from this method is limited only by the predefined cutoff distance R_c, which can be checked by increasing the supercell size.

B. Method for computing the derivatives of the symmetric exchange parameters

The above approach considered how to evaluate the exchange parameters for a given structure. We now examine the dependence of the total energy on the atom displacements: $E(\mathbf{u}_1, \ldots, \mathbf{u}_n, \mathbf{S}_1, \ldots, \mathbf{S}_m) = E_0(\mathbf{U}) + \sum_{\langle i,j \rangle} J_{ij}(\mathbf{U}) \mathbf{S}_i \cdot \mathbf{S}_j$, where $\mathbf{U} = (\mathbf{u}_1, \ldots, \mathbf{u}_n)$ and $\mathbf{u}_k$ $(1 \leqslant k \leqslant n)$ denote the displacements of atom k from a reference structure, n and m are the total number of atoms and total number of spin sites in the supercell, respectively. By taking the partial derivative of the above equation with respect to $u_{k\alpha}$, we obtain

$$
\frac{\partial E}{\partial u_{k\alpha}} = \frac{\partial E_0}{\partial u_{k\alpha}} + \sum_{\langle i,j \rangle} \frac{\partial J_{ij}}{\partial u_{k\alpha}} \mathbf{S}_i \cdot \mathbf{S}_j.
\tag{4}
$$

In terms of the same four spin states used for extracting J_{12}, the derivative of J_{12} with respect to $u_{k\alpha}$ is found as

$$
\frac{\partial J_{12}}{\partial u_{k\alpha}} = \frac{1}{4S^2}\left(\frac{\partial E_1}{\partial u_{k\alpha}} + \frac{\partial E_4}{\partial u_{k\alpha}} - \frac{\partial E_2}{\partial u_{k\alpha}} - \frac{\partial E_3}{\partial u_{k\alpha}} \right),
\tag{5}
$$

where $-\frac{\partial E_i}{\partial u_{k\alpha}}$ $(i = 1, \ldots, 4)$ is the force acting on the atom k along the α direction. The force can be computed using the Hellmann-Feynman theorem and is readily available in many standard DFT schemes. From Eq. (5), we can see that the dependence of the exchange parameter J_{12} on all the atom displacements can be computed by performing four static total energy calculations. This means that the calculation of

first-order derivative of the exchange parameter does not require extra calculations if one calculates the exchange parameter using our above method. Therefore, our new approach utilizing the Hellmann-Feynman forces has a great computational advantage over the finite difference method in which each $\frac{\partial J_{12}}{\partial u_{k\alpha}}$ requires several total energy calculations.

C. Methods for computing DM interaction parameters, single-ion anisotropy parameters, and their derivatives

Our method for calculating the symmetric exchange parameter and its derivative can be also extended to compute the antisymmetric DM interaction parameter (**D**) and single-ion anisotropy (SIA) parameter (A) and their derivatives. Let us describe the method of calculating the DM interaction parameter (vector $\mathbf{D_{12}}$) between spin site 1 and spin site 2. Here, we calculate the three components D_{12}^x, D_{12}^y, and D_{12}^z of the DM vector separately for a general system, although sometimes the direction of the DM vector can be determined by the crystal symmetry. Without loss of generality, let us focus on the calculation of D_{12}^z. We consider the following four spin configurations in which the spins 1 and 2 are oriented along the x and y axes, respectively: (i) $\mathbf{S}_1 = (S,0,0)$, $\mathbf{S}_2 = (0,S,0)$, (ii) $\mathbf{S}_1 = (S,0,0)$, $\mathbf{S}_2 = (0,-S,0)$, (iii) $\mathbf{S}_1 = (-S,0,0)$, $\mathbf{S}_2 = (0,S,0)$, (iv) $\mathbf{S}_1 = (-S,0,0)$, $\mathbf{S}_2 = (0,-S,0)$. In these four spin configurations, the spins of all the other spin sites are the same and are along the z direction. The spin interaction energy for the four spin configurations can be written as

$$
E_{\text{spin}} = D_{12}^z S_1^x S_2^y - S_1^x \sum_{i \neq 1,2} D_{1i}^y S_i^z + S_2^y \sum_{i \neq 1,2} D_{2i}^x S_i^z + E_{\text{other}}.
\tag{6}
$$

As in the case of the symmetric exchange, we have

$$
\begin{aligned}
D_{12}^z &= \frac{1}{4S^2}(E_1 + E_4 - E_2 - E_3), \\
\frac{\partial D_{12}^z}{\partial u_{k\alpha}} &= \frac{1}{4S^2}\left(\frac{\partial E_1}{\partial u_{k\alpha}} + \frac{\partial E_4}{\partial u_{k\alpha}} - \frac{\partial E_2}{\partial u_{k\alpha}} - \frac{\partial E_3}{\partial u_{k\alpha}} \right).
\end{aligned}
\tag{7}
$$

Since the DM interaction is a consequence of spin-orbit coupling (SOC), it is necessary that the energies of the four ordered spin states be determined by DFT calculations with SOC effects taken into consideration. The other two components D_{12}^x and D_{12}^y can be computed in a similar manner. This is a general method to compute both the direction and the magnitude of a DM interaction parameter. For the calculation of the single-ion anisotropy parameter, we consider the spin site 1. If the spin has an easy-axis (with local z' axis) or easy-plane anisotropy, the single-ion anisotropy term can be expressed as $H_{\text{sia}} = A_1 S_{z'}^2$. To evaluate A_1, we consider the four spin states in which the spin directions for site 1 are along z', $-z'$, x', and $-x'$ with the spins at all the other spin sites along the y direction. One can easily find that $A_1 = \frac{E_1 + E_2 - E_3 - E_4}{2S^2}$ and $\frac{\partial A_1}{\partial u_{k\alpha}} = \frac{1}{2S^2}\left(\frac{\partial E_1}{\partial u_{k\alpha}} + \frac{\partial E_2}{\partial u_{k\alpha}} - \frac{\partial E_3}{\partial u_{k\alpha}} - \frac{\partial E_4}{\partial u_{k\alpha}} \right)$. Here the total energy calculations should include SOC effects because the single-ion anisotropy is a consequence of SOC.

III. PREDICTION OF THE SPIN-LATTICE ORDER

It was shown that the spin-lattice coupling may lead to a distortion of the lattice to lower the exchange energy and relieve the frustration of a frustrated spin system (the "spin-Teller" effect).[15] How the lattice distorts is determined by the balance between the spin exchange and lattice elastic energies and depends on the parameters of the full spin-lattice coupled Hamiltonian. With the exchange parameters and their first-order derivatives with respect to the atom displacements in hand, one can predict its spin-lattice ground state with a lower crystal symmetry. At high temperature, a magnetically frustrated system is usually in a disordered paramagnetic (PM) state with a high symmetry. We now write the total energy of a frustrated system with the PM state as a reference state:

$$E(\mathbf{u}_1, \ldots, \mathbf{u}_n, \mathbf{S}_1, \ldots, \mathbf{S}_m) = E_{\mathrm{PM}} + E_{\mathrm{ph}} + E_{\mathrm{spin}}, \quad (8)$$

where $E_{\mathrm{ph}} = 1/2 \sum_{ij\alpha\beta} C_{ij}^{\alpha\beta} u_{i\alpha} u_{j\beta}$ is the phonon Hamiltonian ($C_{ij}^{\alpha\beta}$ is the force constant) and $E_{\mathrm{spin}} = \sum_{\langle i,j \rangle} [J_{ij}(\mathbf{U})\mathbf{S}_i \cdot \mathbf{S}_j + \mathbf{D}_{ij}(\mathbf{U}) \cdot (\mathbf{S}_i \times \mathbf{S}_j)] + \sum_i A_i(\mathbf{U})S_{iz'}^2$. Here $J_{ij}(\mathbf{U}) = J_{ij}^0 + \sum_{k\alpha} \frac{\partial J_{ij}}{\partial u_{k\alpha}} u_{k\alpha}$, J_{ij}^0, and $\frac{\partial J_{ij}}{\partial u_{k\alpha}}$ are computed using the PM structure. We have similar expressions for $\mathbf{D}_{ij}(\mathbf{U})$ and $A_i(\mathbf{U})$. The particular lattice distortion leading to the lowest energy for a given spin configuration can be obtained by solving the following linear equations:

$$\frac{\partial E}{\partial u_{k\alpha}} = \sum_{j\beta} C_{kj}^{\alpha\beta} u_{j\beta} + \frac{\partial E_{\mathrm{spin}}}{\partial u_{k\alpha}} = 0, \quad (9)$$

where $1 \leqslant k \leqslant n$ and $\alpha = 1, 2, 3$. The lowest energy for a given spin configuration can then be calculated by using Eq. (8). The spin-lattice ground state can be found by comparing the energies of different spin configurations.

IV. APPLICATION TO MGCR$_2$O$_4$

A. Computational details of DFT calculations

Our total energy calculations are based on the DFT plus the on-site repulsion (U) method[16] within the local density approximation (LDA+U) on the basis of the projector augmented wave method[17] encoded in the Vienna *ab initio* simulation package.[18] We used the on-site repulsion $U = 3$ eV and the exchange parameter $J = 0.9$ eV on Cr, which reproduce the dominant features of the photoemission and band gap data in sulfur Cr^{3+} spinels.[13] The plane-wave cutoff energy was set to 400 eV.

B. Exchange parameters and their derivatives

We now apply the above method to calculate the exchange parameters and their derivatives of $MgCr_2O_4$[19] to find its spin-lattice coupled ground state. $MgCr_2O_4$, which crystallizes in a normal spinel structure with the Cr^{3+} ions ($S = 3/2$) forming a pyrochlore lattice [see Fig. 1(a)], is strongly frustrated due to the strong AFM interactions between the NN Cr^{3+} spins. We consider first the $MgCr_2O_4$ structure optimized with the FM spin state. The optimized lattice constant is 8.277 Å. We calculate all symmetric spin exchange interactions up to the fourth NN pairs [see Fig. 1(a)] using a $2 \times 2 \times 2$ supercell
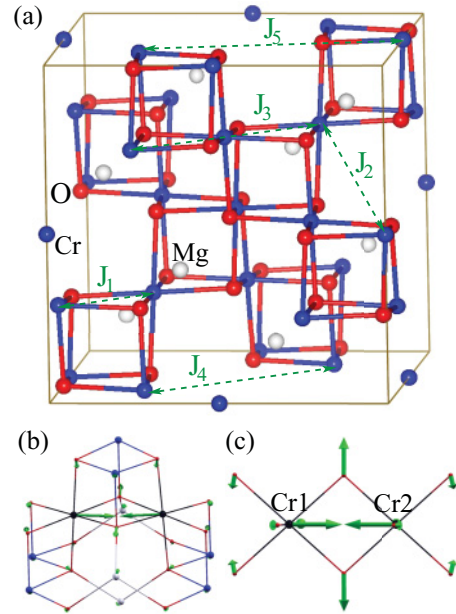

FIG. 1. (Color online) (a) Structure of $MgCr_2O_4$ and exchange paths. [(b) and (c)] The side and top views of the derivative of the NN exchange J_1 with respect to the atom displacements.

of the $MgCr_2O_4$ conventional cubic cell; the NN exchange J_1 within each Cr_4 tetrahedron and the farther NN exchanges J_2, J_3, J_4, and J_5. We find that $J_1 = 4.56$, $J_2 = 0.01$, $J_3 = 0.26$, $J_4 = 0.08$, and $J_5 = -0.01$ meV. The NN exchange J_1 is strongly AFM while all next NN exchange interactions are almost negligible.

Using Eq. (5), we calculate the derivatives of the exchange parameters with respect to atom displacements using the optimized FM structure. Our results show the NN exchange J_1 depends strongly on the positions of those atoms shown in Figs. 1(b) and 1(c). In particular, the largest derivative $|\frac{\partial J_1}{\partial \mathbf{u_k}}|$ of the exchange interaction between two NN Cr ions occurs when site k is one of two Cr ions (we hereafter refer to this vector as $\mathbf{J}'_{1\mathrm{Cr}}$). When the two Cr ions move close to each other, the NN exchange J_1 increases. The magnitude of the derivative is as large as 43.40 meV/Å, which is close to the value (40.25 meV/Å) extracted by the finite difference method. This can be understood because when the distance between two Cr ions becomes short, the direct overlap between the t_{2g} orbitals of the two Cr^{3+} (d^3) ions becomes stronger. The NN exchange J_1 also depends substantially on the positions of the two bridging oxygen atoms with its derivative approximately along the direction from the midpoint of the two NN Cr ions to the oxygen ion (hereafter this vector is referred to as $\mathbf{J}'_{1\mathrm{O}}$). We find the direction of $\mathbf{J}'_{1\mathrm{O}}$ is due to the fact that the antibonding repulsion between O p orbital and Cr t_{2g} orbitals becomes weaker and the t_{2g} orbitals of the two Cr^{3+} (d^3) ions can have a better overlap if the bridge O atoms move away from the Cr-Cr pair. Another possible explanation is that the increased Cr-O distance might result in a smaller FM contribution, enhancing the overall AFM coupling. The derivatives of other symmetric exchange parameters are found to be vanishingly small.

It was suggested that the DM interaction might be relevant to the spin-lattice order in a similar system.[20] As expected from the symmetry analysis, the DM vector for a Cr-Cr edge

of each Cr_4 tetrahedron is perpendicular to the Cr-Cr bond and is parallel to the opposite edge of the Cr_4 tetrahedron. Using our method, we find the magnitude of the DM parameter to be 0.03 meV (0.7% of J_1). We have checked that our method is accurate enough to predict reliable DM vectors. And the derivative of the DM parameter with respect to the Cr ion position of the Cr-Cr pair has the largest magnitude of 0.41 meV/Å. Our calculations show that the Cr^{3+} ion has an easy plane anisotropy with the plane perpendicular to the threefold rotational axis z'. The calculated SIA parameter is -0.05 meV (1.1% of J_1) and the largest derivative of the SIA is 0.18 meV/Å. Our first-principles calculation established that, for $MgCr_2O_4$, the DM parameter, SIA parameter, and their derivatives are negligible compared to NN J_1.

C. Spin-lattice ground state of $MgCr_2O_4$

At high temperature, $MgCr_2O_4$ is paramagnetic (PM) with a cubic symmetry. To simulate the PM state, we use a special quasirandom structure (SQS)[21] spin configuration. The magnetic unit cell of the SQS spin configuration is four times as large as the chemical unit cell of $MgCr_2O_4$. Then we fix the lattice constant to that (8.259 Å) of the SQS structure and relax the internal atomic coordinates with the FM spin configuration. In this way, we can get approximate exchange parameters J_{ij}^0 (4.80 meV), their derivative $\frac{\partial J_{ij}}{\partial u_{k\alpha}}$ ($|\mathbf{J}'_{1Cr}| = 49.11$ meV/Å and $|\mathbf{J}'_{1O}| = 25.15$ meV/Å), and the force constants $C_{ij}^{\alpha\beta}$ appropriate for the PM state. The differences between the force constants of the FM state and those of the PM state are small because they are of second-order effect and, thus, are neglected in this work. All these parameters are necessary in finding the spin-lattice coupled ground state of $MgCr_2O_4$ by solving Eq. (9). The force constants are obtained by finite difference as in phonon calculations by the direct method. The force constants are considered fixed and independent of the atomic displacement.

Our calculations show that the dominant exchange interaction in $MgCr_2O_4$ is the NN AFM symmetric exchange interaction J_1. For the Heisenberg Hamiltonian with the NN exchange interaction J_1 on the pyrochlore lattice ($H_{NN} = \sum_{\langle NN i,j \rangle} J_1 \mathbf{S}_i \cdot \mathbf{S}_j$), the degeneracy of the spin ground state is macroscopic: If for any of the Cr tetrahedra the sum of the four spins is zero, then it is a spin ground state.[15] We will use our calculated parameters (not only the exchange parameter but also its derivatives) and solve the full spin-lattice coupled Hamiltonian to determine the ground state of $MgCr_2O_4$. As a first step, we consider the case where the spin-lattice ground state has the same size as the primitive chemical unit cell. In this case, we can easily generate a spin configuration[15] that is one of the highly degenerate spin ground states of the Heisenberg Hamiltonian H_{NN}. We generate 2000 such spin configurations and calculate the energy of the spin-lattice coupled system to find that the spin configuration shown in Fig. 2 has the lowest energy and, thus, is the ground state of the spin-lattice coupled Hamiltonian. The spin state is collinear with two up spins and two down spins. To confirm the above prediction from the model Hamiltonian analysis, we carry out DFT calculations to optimize both the lattice parameters and the internal coordinates of $MgCr_2O_4$ with the collinear AFM spin state. The relaxed (i.e., distorted)
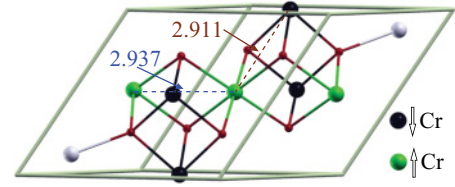

FIG. 2. (Color online) The ground state of $MgCr_2O_4$ by considering the full spin-lattice coupled Hamiltonian. The numbers (in Å) denote the Cr-Cr distances. The exchange parameter for the Cr-Cr pair with the 2.911 Å distance is 5.47 meV, while the exchange parameter for the Cr-Cr pair with the 2.937 Å distance is 3.84 meV.

structure is calculated to have a lower energy by 6.33 meV/Cr than the unrelaxed structure with the same collinear AFM spin state. In the relaxed structure, the distance between NN spin up Cr^{3+} ion and spin down Cr^{3+} ion is smaller by 0.026 Å than that between NN Cr^{3+} ions with the same spin direction. The exchange parameters for the two different Cr-Cr exchange interactions are 5.47 and 3.84 meV, respectively, to be compared with the value (4.80 meV) for the undistorted structure. This difference is due to the spin-lattice coupling, which makes the exchange parameter between AFM (FM) coupled spins larger (smaller). The relaxed $MgCr_2O_4$ structure is tetragonal (space group $I4_1/amd$, No. 141) with $a = 5.873$ Å and $c = 8.160$ Å. Experimentally, the spinel $MgCr_2O_4$ was found to undergo a sharp first-order transition at $T_N = 12.4$ K from a cubic paramagnetic phase (space group $Fd\bar{3}m$) to a tetragonal antiferromagnetically ordered structure ($I4_1/amd$, $a = 5.8961$Å and $c = 8.3211$ Å at 10 K).[19] Our first-principles result thus confirms the $I4_1/amd$ space group of the ground state of $MgCr_2O_4$ and $c < \sqrt{2}a$ below T_N. It should be noted that our work predicts a collinear AFM ground state with the propagation vector $\mathbf{q} = (0,0,0)$ with respect to the tetragonal lattice, in contrast to the previously proposed noncollinear magnetic models.[19,22] This calls for further ultralow temperature experiments to verify our prediction.

V. CONCLUSION

In summary, we proposed a general and efficient method to quantitatively describe spin-lattice coupling. This method allows one to evaluate each spin exchange (and DM interaction) as well as its derivatives with respect to atom displacements on the basis of DFT calculations for four ordered spin states. By applying this method to the spin-frustrated spinel $MgCr_2O_4$, we showed that it undergoes a structural transition from the cubic to a tetragonal structure with collinear AFM spin configuration. Our method provides an efficient first-principles way of describing the interplay between spin order and lattice distortion in frustrated magnetic systems.

*hxiang@fudan.edu.cn

[1] J. S. Gardner, M. J. P. Gingras, and J, E. Greedan, Rev. Mod. Phys. **82**, 53 (2010).

[2] L. Balents, Nature **464**, 199 (2010).

[3] T. E. Saunders and J. T. Chalker, Phys. Rev. B **77**, 214438 (2008); G.-W. Chern, C. J. Fennie, and O. Tchernyshyov, *ibid.* **74**, 060405 (2006).

[4] S.-W. Cheong and M. Mostovoy, Nat. Mater. **6**, 13 (2007); R. Ramesh and N. Spaldin, *ibid.* **6**, 21 (2007).

[5] T. Kimura, T. Goto, H. Shintani, K. Ishizaka, T. Arima, and Y. Tokura, Nature **426**, 55 (2003)

[6] N. Hur, S. Park, P. A. Sharma, J. S. Ahn, S. Guha, and S-W. Cheong, Nature **429**, 392 (2004).

[7] L. C. Chapon, G. R. Blake, M. J. Gutmann, S. Park, N. Hur, P. G. Radaelli, and S.-W. Cheong, Phys. Rev. Lett. **93**, 177402 (2004).

[8] I. A. Sergienko and E. Dagotto, Phys. Rev. B **73**, 094434 (2006).

[9] A. Malashevich and D. Vanderbilt, Phys. Rev. Lett. **101**, 037210 (2008).

[10] H. J. Xiang, Su-Huai Wei, M.-H. Whangbo, and Juarez L. F. Da Silva, Phys. Rev. Lett. **101**, 037209 (2008).

[11] G. Lawes *et al.*, Phys. Rev. Lett. **95**, 087205 (2005).

[12] M. Mochizuki, N. Furukawa, and N. Nagaosa, Phys. Rev. Lett. **105**, 037205 (2010).

[13] C. J. Fennie and K. M. Rabe, Phys. Rev. Lett. **96**, 205505 (2006).

[14] M.-H. Whangbo, H.-J. Koo, and D. Dai, J. Solid State Chem. **176**, 417 (2003).

[15] O. Tchernyshyov, R. Moessner, and S. L. Sondhi, Phys. Rev. Lett. **88**, 067203 (2002); Phys. Rev. B **66**, 064403 (2002).

[16] A. I. Liechtenstein, V. I. Anisimov, and J. Zaanen, Phys. Rev. B **52**, R5467 (1995).

[17] P. E. Blöchl, Phys. Rev. B **50**, 17953 (1994); G. Kresse and D. Joubert, *ibid.* **59**, 1758 (1999).

[18] G. Kresse and J. Furthmüller, Comput. Mater. Sci. **6**, 15 (1996); Phys. Rev. B **54**, 11169 (1996).

[19] L. Ortega-San-Martín, A. J. Williams, C. D. Gordon, S. Klemme, and J. P. Attfield, J. Phys. Condens. Matter **20**, 104238 (2008).

[20] S. Ji, S.-H. Lee, C. Broholm, T. Y. Koo, W. Ratcliff, S.-W. Cheong, and P. Zschack, Phys. Rev. Lett. **103**, 037201 (2009).

[21] A. Zunger, S.-H. Wei, L. G. Ferreira, and James E. Bernard, Phys. Rev. Lett. **65**, 353 (1990); S.-H. Wei, L. G. Ferreira, James E. Bernard, and A. Zunger, Phys. Rev. B **42**, 9622 (1990).

[22] Shaked, J. M. Hastings, and L. M. Corliss, Phys. Rev. B **1**, 3116 (1970).